Vol. 92 No. 6 pp. 2405–2415 ACTA GEOLOGICA SINICA (English Edition) Dec. 2018

Reviews

Assessing Lateral Continuity within the Yammama Reservoir in the Foroozan Oilfield, Offshore Iran: An Integrated Study

Payam HASSANZADEH[1], Ahmad Reza RABBANI[1, *], Ardeshir HEZARKHANI [2] and Saeed KHAJOOIE[3]

1 *Department of Petroleum Engineering, Amirkabir University of Technology, Hafez Ave. No. 424, Tehran, Iran*

2 *Department of Mining and Metallurgy Engineering, Amirkabir University of Technology, Hafez Ave. No. 424, Tehran, Iran*

3 *Department of Reservoir Engineering, Exploration Directorate of National Iranian Oil Company (NIOC-EXP), Tehran, Iran*

Abstract: Located in Iranian sector of the Persian Gulf, Foroozan Oilfield has been producing hydrocarbons via seven different reservoirs since the 1970s. However, understanding fluid interactions and horizontal continuity within each reservoir has proved complicated in this field. This study aims to determine the degree of intra-reservoir compartmentalization using gas geochemistry, light hydrocarbon components, and petroleum bulk properties, comparing the results with those obtained from reservoir engineering indicators. For this purpose, a total of 11 samples of oil and associated gas taken from different producing wells in from the Yammama Reservoir were selected. Clear distinctions, in terms of gas isotopic signature and composition, between the wells located in northern and southern parts of the reservoir (i.e. lighter $\delta^{13}C_1$, lower methane concentration, and negative sulfur isotope in the southern part) and light hydrocarbon ratios (e.g. nC_7/toluene, 2,6-dmC_7/1,1,3-tmcyC_5 and m-xylene/4-mC_8) in different oil samples indicated two separate compartments. Gradual variations in a number of petroleum bulk properties (API gravity, V/Ni ratios and asphaltene concentration) provided additional evidence on the reservoir-filling direction, signifying that a horizontal equilibrium between reservoir fluids across the Yammama Reservoir is yet to be achieved. Finally, differences in water-oil contacts and reservoir types further confirmed the compartmentalization of the reservoir into two separate compartments.

Key words: reservoir compartmentalization, gas geochemistry, light hydrocarbons, reservoir engineering, Yammama Reservoir, Foroozan Oilfield, Iran

1 Introduction

Application of geochemistry for solving engineering problems such as reservoir compartmentalization has been well documented in recent years (Kaufman et al., 1990; England et al., 1995, England, 2007). Light hydrocarbon components of petroleum have been used to assess reservoir continuity. Comparing inter-paraffin peak ratios from C_5-C_9 n-alkanes on a low-molecular weight hydrocarbon chromatogram has been seen to contribute to delineation of reservoir continuity (Márquez et al., 2016). Another tool for identifying different reservoir segments is gas geochemistry. Typically, continuous reservoirs exhibit similar gas compositions and isotopic signatures (Schoell et al., 1993; Márquez et al., 2013), so that reservoir compartmentalization can be indicated using differences in composition and isotopic signatures of gas samples within a reservoir. Alongside the mentioned methods, formation pressure measurements are helpful in identifying horizontal and vertical reservoir continuities (Páez et al., 2010). Faults or reservoir pinchouts may only bound three sides of a compartment. In some cases, oil may become separated across a fault and a separate gas-oil contact (GOC) and/or water-oil contact (WOC) may develop, thus defining two different compartments (Vrolijk et al., 2005)

Different authors have presented a variety of methods for assessing reservoir continuity, e.g., geochemical fingerprinting (Kaufman et al., 1990; Hwang and Baskin,

* Corresponding author. E-mail: Rabbani@aut.ac.ir

1994; Smalley and Hale, 1996), gas geochemistry (Beeunas et al., 1999; Levaché et al., 2000; Rein and Schulz, 2007; Márquez et al., 2013), formation water analysis (Gill et al., 2010), structural and stratigraphic continuity (Hovadik and Larue, 2010), formation pressure test (Páez et al., 2010) and FTIR and SUVF spectroscopy (Permanyer et al., 2002; Permanyer et al., 2007). However, to the best of our knowledge, integrated approaches for assessing reservoir continuity using a combination of organic geochemistry tools (e.g. gas geochemistry, high-resolution GC, and bulk petroleum properties) with reservoir engineering evidence, is yet to be introduced.

The first objective of this study was to assess reservoir continuity by combining low-cost yet quick geochemical techniques with reservoir engineering data within the Yammama Reservoir in Foroozan Oilfield (Persian Gulf). The second objective was to define reservoir-filling direction based on geochemical data, so as to help future well-emplacement and reservoir production management. Trying to accomplish the objectives, gas fingerprinting data (composition and isotopic signatures of different gas components), high-resolution GC results and bulk petroleum properties (API gravity, asphaltene content and V/Ni ratio) were analyzed on a total of 11 oil and associated gas samples taken from the reservoir. In addition, water-oil contact (WOC) and reservoir type were determined based on pressure measurements at different parts of the Yammama Reservoir, with the results compared to those derived from geochemical analysis.

2 Geological Setting

Discovered in 1966, Foroozan Oilfield lies about 100 km to the southwest of Kharg Island in the Persian Gulf, straddling the sea border with Saudi Arabia. As an extension of Saudi Arabia's Marjan Field (Fig. 1a), this field has been in production since 1974.

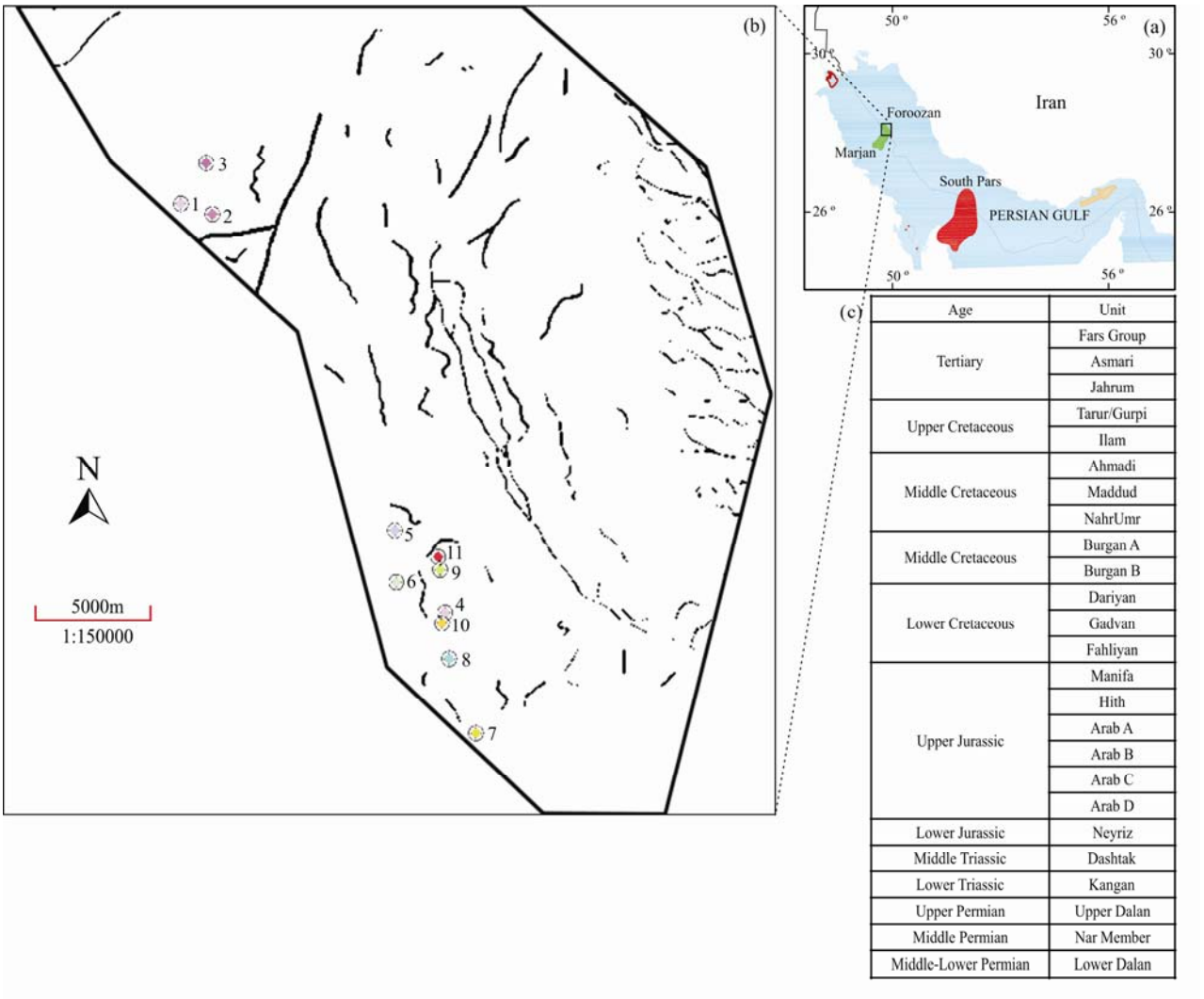

(c)

Age	Unit
Tertiary	Fars Group
	Asmari
	Jahrum
Upper Cretaceous	Tarur/Gurpi
	Ilam
Middle Cretaceous	Ahmadi
	Maddud
	NahrUmr
Middle Cretaceous	Burgan A
	Burgan B
Lower Cretaceous	Dariyan
	Gadvan
	Fahliyan
Upper Jurassic	Manifa
	Hith
	Arab A
	Arab B
	Arab C
	Arab D
Lower Jurassic	Neyriz
Middle Triassic	Dashtak
Lower Triassic	Kangan
Upper Permian	Upper Dalan
Middle Permian	Nar Member
Middle-Lower Permian	Lower Dalan

Fig. 1. (a), Location map of the Foroozan Oilfield in the Persian Gulf, Iran; (b), sampled wells with respect to fault distribution, and (c) stratigraphic column.

The field lies on the northeastern flank of a very large domal anticline. Similar to other large domal anticlines in the Persian Gulf region, Foroozan structure is known to be formed by halokinesis of the underlying Hormoz Salt during early Cenozoic. The salt movement has developed very gentle anticlines with intervening salt withdrawals and fault-collapsed synclines.

The Foroozan Oilfield is well-known for its particular complexities, making it very difficult to determine reservoir-filling history for such a complex field. Structural/stratigraphic barriers have divided Foroozan Oilfield into five different segments (F1, F2, F3, F5 and F8), which are producing from seven different reservoirs. The distribution of faults across the Yammama Reservoir is shown in Figure 1b.

The Azadegan sandstone, a member of the Kazhdumi Formation (equivalent to Burgan Member), and Fahliyan Formation (equivalent to the Yammama Formation) form two main reservoirs in the Foroozan Oilfield. The Azadegan sandstone is divided into a lower massive sandstone unit (designated as Burgan B) and an upper unit with higher shale content (designated as Burgan A). Dated back to Neocomian stage and exhibiting a clean limestone succession, the Yammama Formation is the oldest Cretaceous oil-bearing reservoir in Foroozan Oilfield.

Additional reservoirs in Foroozan Oilfield include carbonates of the Lower Cretaceous Dariyan (equivalent to Shuaiba), and the Upper Jurassic Manifa Member and Surmeh Formation (equivalent to Arab Members) (Fig. 1c).

3 Material and Methods

A total of 11 oil samples were collected from 11 wells drilling into the Yammama Reservoir in Foroozan Oilfield. Moreover, 11 samples of associated gas were further taken from the 11 wells in IsoTube containers by means of a pressure regulator connected to a surface separator at well-head. All of the sampled wells were in production from the Yammama Reservoir, a saturated oil reservoir. Figure 1b shows the sampled wells in the field with respect to fault distributions throughout the entire reservoir. The methods used in this study are described in the following sections.

3.1 Gas composition analysis

The associated gas samples were analyzed for their hydrocarbon composition in terms of C_1-C_6 contents by a GC 8000 series equipped with split/splitless injector and flame ionization detector (GC-FID) with a PORAPLOT N capillary column, and their permanent gas composition (H_2S, N_2, O_2, CO_2, CO, H_2 and He) by GC-TCD with MOLSIEVE and PORAPLOT N capillary columns on a Shimadzu GC-2014 machine. Measurement uncertainty associated with the determination of the gas compounds was found to range from 5 to 10 relative %, depending on the absolute value of the compound in question.

3.2 Low molecular weight hydrocarbon analysis

Analysis of low molecular weight hydrocarbons C_5 to C_9 was performed utilizing a Fisons Instrument GC 8000 series equipped with split/splitless injector and flame ionization detector (FID) equipped with a Zebron ZB-1 HT Inferno fused silica column (Phenomenex®, length: 30 m, internal diameter: 0.25 mm, film thickness: 0.25 μ). GC analysis was initiated with an injector temperature of 270ºC; split injection was then performed at 80ºC, increasing the temperature to 150ºC at 2 ºC/min and then to 310ºC at 3 ºC/min, where it was held for 20 minutes. Hydrogen was used as a carrier gas at a velocity of about 40 cm/s.

3.3 Continuous flow isotope ratio analysis (CF-IRMS) $^{13}C/^{12}C$, $^{15}N/^{14}N$ and D/H

Continuing with the research, $^{13}C/^{12}C$, $^{15}N/^{14}N$ and D/H isotope analyses were performed by a PDZ EUROPA 2020 CF-IRMS. The gas chromatographic system used in the isotopic analyses was a Hewlett-Packard HP 9890 Series II equipped with a 10 m-long 16" SS-tube filled with Shin Carbon, with helium 6.0 serving as a carrier gas. In each round of the analyses, the temperature was programmed to be held at 70°C for 5 min and then increased to 320°C at 22°C, where it was held for 20 min. According to the results, uncertainties associated with $\delta^{13}C$ and $\delta^{15}N$ values were found to be better than ±0.3‰. The reproducibility of the δD values was around ±2‰.

3.4 S-34 isotope analysis by EA-IRMS

The sulfur isotopic composition of the associated gas samples were measured using a Flash HT 2000 Elemental Analyzer (Thermo Scientific) equipped with combustion and pyrolysis furnaces and coupled with a Delta V Advantage IRMS (Thermo Scientific) ion source, which was capable of performing GC analysis. The value of $\delta^{34}S$ for each sample was measured twice and the mean value was reported.

3.5 Elemental composition (Ni, V)

The Ni and V measurements were performed through application of an ICP-MS system. The system consisted of a Metrohm 709 IC pump, a Metrosep® C4/4.0 250 mm cation exchange column with a C4 GC/4.0 guard column, and a PerkinElmer DRC equadrupole ICP-MS with a quartz glass cyclone spray chamber combined with a

Meinhard nebuliser.

3.6 API measurement

Applying ASTM D-4052 standard method (ASTM, 2011), API gravities of the oil samples were measured. For this purpose, a small volume (~0.7 ml) of the oil sample was introduced into an oscillating sample tube. Accordingly, the change in oscillation frequency caused by the change in the mass of the tube was used in combination with calibration data to determine the sample density.

4 Results and Discussion

4.1 Gas composition and isotopic signatures

The composition and isotopic signatures of the gas samples are given in Table 1. The concentration of methane, as the main constituent of the gas samples, was found to vary from 62-64% in the northwestern part to 75–77% in the southeastern part of the reservoir, indicating a clear lateral distinction. The contents of other gas components, such as ethane, propane and butane, also exhibited such a clear distinction. Based on the results, the average concentration of ethane over the samples taken from the northwestern part of the reservoir was 9.9%, while the corresponding concentration in the samples taken from the southeastern part of the reservoir was 3.1%. The corresponding average concentrations for propane and butane were 2.3% and 1.04%, and 0.65% and 0.39%, respectively. These clear differences in the gas composition suggest lateral heterogeneity across the reservoir. Non-hydrocarbon gases were found to consist mainly of carbon dioxide, hydrogen sulfide and nitrogen. Carbon dioxide and nitrogen concentrations showed no particular differences throughout the entire reservoir. Conversely, hydrogen sulfide concentration was found to increase as one moved from the north to the south of the reservoir (on average, from 0.68% in the north to 2.37% in the south), further emphasizing the lack of homogeneity throughout the Yammama Reservoir. Based on the petroleum engineering data, reservoir pressure was uniform across the Yammama Reservoir (3250 psi). Therefore, being dependent on the reservoir pressure, the solubility of hydrocarbon gases and hydrogen sulfide in the oil were concluded to be constant throughout the reservoir.

The content of stable isotopes of different components of the gas samples are reported in Table 2. With the increase in alkane gas carbon number, the stability of its carbon isotopes make stronger, which is one of the most commonly used and most effective geochemical indexes with which to evaluate the genesis type of natural gas, gas

Table 1 Gas composition (%) of the samples taken from the Yammama Reservoir in the Foroozan Oilfield

Well No.	C_1	C_2	C_3	nC_4	iC_4	Wetness	N_2	CO_2	H_2S
1	62	17	9.2	2	0.59	31.7	0.6	4.5	1.3
2	64	17	9.5	2.3	0.61	31.5	0.8	3.5	0.43
3	62	17	11	2.3	0.74	33.6	0.7	3.3	0.32
4	77	7.3	3	1	0.39	13.2	0.8	5.3	2.4
5	75	7.9	3	1.1	0.37	14.2	0.7	5.3	3
6	76	7.3	3	1.1	0.38	13.4	0.6	5.3	3
7	77	7.2	3	0.98	0.4	13.1	0.7	4.9	1.9
8	76	8.1	3.3	1.1	0.41	14.5	0.7	5.4	2.2
9	77	7.2	3	1	0.38	13.1	0.8	5	1.9
10	76	8	3.3	0.95	0.42	14.6	1.1	4.4	1.6
11	75	7.6	3.1	1.1	0.4	14	0.8	5.2	3

Table 2 $\delta^{13}C$ (‰), δD (‰), $\delta^{15}N$ and $\delta^{34}S$ (‰) values in different components of the gas samples taken from Yammama Reservoir

Well No.	$\delta^{13}C_1$	$\delta^{13}C_2$	$\delta^{13}C_3$	$\delta^{13}iC_4$	$\delta^{13}nC_4$	δDC_1	$\delta^{13}CO_2$	$\delta^{15}N$	$\delta^{34}S$
1	−58.9	−43.6	−32.6	−32.2	−28.2	−304	−3.4	−2.1	−11.1
2	−56.2	−44.1	−33.4	−32.7	−28.4	−281	−4	−3.5	−10
3	−56.5	−44.1	−33.4	−31	−28.6	−287	−3.6	−2.8	−10
4	−47.4	−34.9	−29.4	−28.1	−25.1	−198	−3.6	−3.7	11
5	−47.7	−34.9	−29.3	−28.5	−24.6	−197	−2.5	−2.5	11.6
6	−47.3	−35.2	−29.9	−30.6	−25.9	−196	−3.8	−3.2	11.2
7	−48.6	−34.4	−29.3	−27.3	−25.1	−194	−2.9	−3.5	11.3
8	−47.5	−33.7	−29	−28.9	−25.3	−197	−2.9	−3.3	10.2
9	−47.1	−34.4	−29.5	−26.9	−25.6	−196	−2.8	−3.9	10.1
10	−47.7	−34.3	−29.4	−29.1	−25.6	−199	−3.3	−2.8	10.3
11	−46.9	−35	−29	−28.1	−25.7	−199	−3	−2.9	12

to gas correlation, and natural gas sources identification (Xie et al., 2017). Carbon isotopic composition of methane at wells 1 to 3 ranged from −56.5‰ to −58.9‰, while that of the remaining wells changed from −46.9‰ to −48.6‰ (Table 2). Lighter carbon isotopes were observed in the methane content of the gas samples taken from the northwestern part of the reservoir rather than the southeastern part of the reservoir; the same was the case for the ethane, propane and butane components of the gas samples. Such a difference in isotopic composition suggested that the faults had the properties of seals, preventing fluid connectivity across the Yammama Reservoir. Moreover, δDC_1 provided additional information about lateral segmentation within the Yammama Reservoir. While δDC_1 values of the wells located in the southeastern part of the reservoir showed a narrow range of −194 to −199‰, the well Nos. 1, 2 and 3 indicated higher values of δDC_1 (−281‰ to −304‰). These results further supported the previously mentioned differences in chemical composition (for methane and other components) between the gas samples taken from the northwestern and southeastern parts of the reservoir, thereby demonstrating the presence of isolated reservoir segments.

The sulfur isotopic composition of the studied gas samples also supported the model of such a compartmentalization in the Yammama Reservoir. Gas samples from the northern sector demonstrated negative

values of sulfur isotopes ranging from −10‰ to −11.1‰, whereas positive values were observed in the southern sector, across the range 10.1‰−12‰. In a carbonate reservoir, H_2S gas can be produced via thermochemical sulfate reduction (TSR) and is controlled by the reservoir temperature and the form of anhydrite present (Worden et al., 1995, 2000). Recent studies have shown that the TSR process starts at temperatures between 127 and 14 ºC, depending on the type of hydrocarbons in the reservoir, and that higher temperatures are required to initiate TSR for methane, rather than heavier hydrocarbons (Machel et al., 1995; Worden et al., 1995; Rooney, 1996). During the TSR process, ^{32}S is firstly produced, due to the requisite bond energy (Zhu et al., 2005). Then, the generated H_2S becomes progressively heavier isotopically as the process goes on. Regarding the reservoir temperature at different wells in the Yammama Reservoir (96.8 to 103ºC) and the results of burial history modeling, which revealed a maximum paleotemperature of 110ºC (Internal Report of the Exploration Directorate of the NIOC, 2017), a thermochemical sulfate reduction process (TSR) was unlikely to occur in the Yammama Reservoir. In addition, being mainly composed of carbonates, the reservoir lithology was poor in evaporates. Therefore, the required conditions for the TSR process to occur were found to be absent in the Yammama Reservoir.

The temperature of the Dehram gas reservoir (Permo-Triassic) was found to vary from 136.6 to 153.3ºC in the field. Separating upper Dalan from lower Dalan in the Dehram Group, the Nar Member exhibited a variable sulfur isotopic signature changing over 11.3‰ to 12.2‰ at different wells across the Persian Gulf, closely resembling the values for the analyzed gas samples (Internal Report of the Exploration Directorate of the NIOC, 2012). Combining all of the available evidence, the TSR process was found to occur in Dehram Reservoir before gas migrates from the Permo-Triassic reservoir to the shallower Yammama Reservoir in the southern part of the field, via faults acting as conduits. Thus, the larger content of methane and the heavier carbon isotopic composition of the gas components in this part of the field can be attributed to the migration of dryer gas from the Dehram reservoir to the southeastern part of the field. The presently occurring H_2S in the northern part of the Yammama Reservoir was most probably generated as a result of kerogen decay.

Regarding methane concentrations and $\delta^{13}C_1$ values in different gases (Schoell, 1983), all of the studied gas samples were classified under thermal oil and exhibited two different groups in terms of degree of maturity and wetness ratio (Fig. 2a). Including well Nos. 1, 2 and 3 (the northwestern part of the reservoir), the first group showed lower maturity, with wetness ratios ranging between 31.5 and 33.6%; whereas the second group encompassed other wells located in the southeastern part of the reservoir with further maturity, and wetness ratios ranging from 13.1 to 14.6%. According to Whiticar et al. (1986) and Hill et al. (2007), the heavier $\delta^{13}C$ values obtained for the well No. 4 to 11 might be due to an increase in the degree of maturity of the source rock. Moreover, application of natural gas plots suggested by Chung et al. (1988) approved the two groups of gases in the Yammama Reservoir (Fig. 2b). Differences in the average carbon isotopic signatures of methane, ethane, propane and butane contents between the gas samples taken from the northwestern and southeastern parts of the field were 10.3‰, 9.3‰, 3.65‰, and 3.03‰ respectively, indicating the presence of different compartments within the Yammama Reservoir.

According to Prinzhofer et al. (2000), a total of 11 chemical and isotopic ratios (C_1/C_2, C_2/C_3, iC_4/nC_4, $\delta^{13}C_1$, $\delta^{13}C_2$, $\delta^{13}C_3$, $\delta^{13}iC_4$, $\delta^{13}nC_4$, $\delta^{13}C_3$-$\delta^{13}C_2$, $\delta^{13}nC_4$-$\delta^{13}iC_4$, and $\delta^{13}C_2$-$\delta^{13}C_1$) were investigated. All of the parameters were found to be positively correlated to maturity; three of the 11 parameters considered herein, namely $\delta^{13}C_3$-$\delta^{13}C_2$, $\delta^{13}nC_4$-$\delta^{13}iC_4$, and $\delta^{13}C_2$-$\delta^{13}C_1$, were positively correlated to the accumulation efficiency, and segregative migration

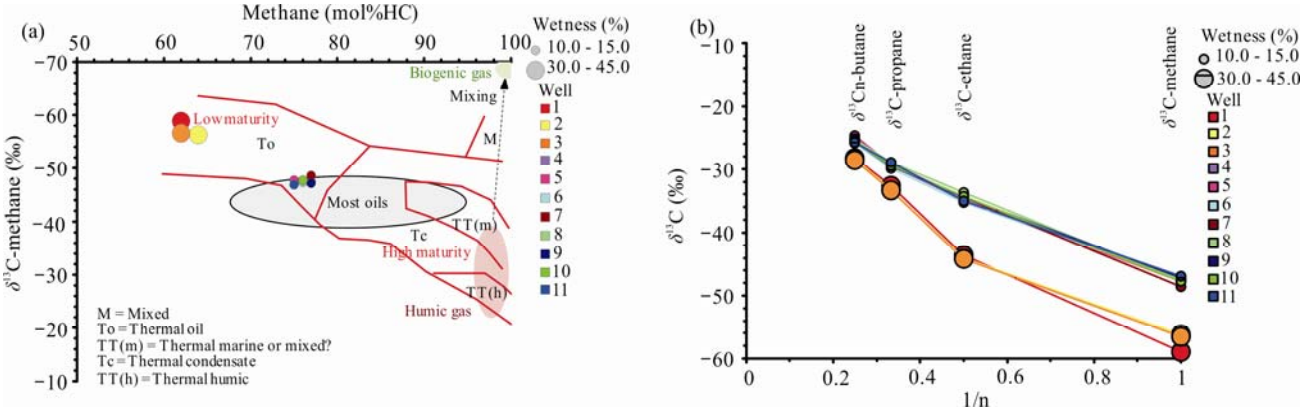

Fig. 2. Plots of $\delta^{13}C_1$ versus methane concentration
(a), $\delta^{13}C$ versus inverse Cnumber; (b), for each of the n-alkanes C_1-C_4 for two different groups of gas samples.

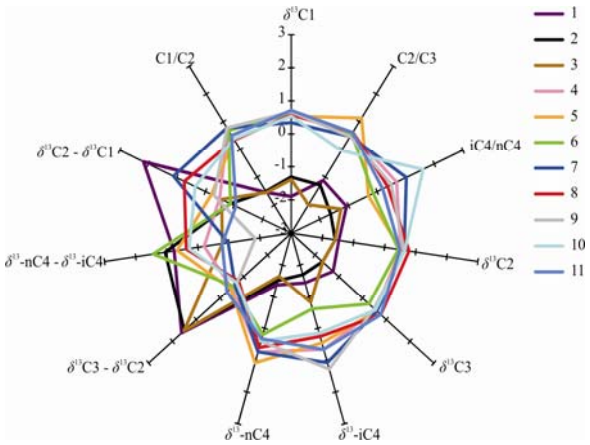

Fig. 3. Normalized Gastar diagram for different gas samples taken from the Yammama Reservoir. The scales are the same for all 11 axes of each Gaster diagram.

might strongly affect the parameters involving methane (positive correlations to C_1/C_2 and $\delta^{13}C_2$-$\delta^{13}C_1$, inverse correlation to $\delta^{13}C_1$). The star diagram (also known as a Gastar diagram) shown in Fig. 3 reveals obvious differences among the gas samples to study the mentioned processes. Two groups of gas samples can be identified based on the Gaster diagram. As expected, the well Nos. 4 through 11 are in the same group, indicating a higher maturity than that observed among the wells located in the northwestern part of the reservoir. A comparison between the two groups of gas samples taken from the Yammama Reservoir shows an increase in accumulation efficiency in a northward direction. These attributes are sufficient to specify two distinct reservoir segments. As a result, it was concluded that the heterogeneities recognized in the star diagrams are signs of geological features that prevent fluid mixing within the Yammama Reservoir.

4.2 A review on biomarkers

From the results of the gas composition analysis, which showed differences in degree of maturity among different gas samples in the northwestern and southeastern parts of the Yammama Reservoir, it was deemed necessary to investigate source rock maturity based on biomarker studies. In addition, source-related biomarker parameters were studied to determine whether one source rock has charged the whole Yammama Reservoir, or different source rocks have provided different parts of the reservoir with hydrocarbons. The m/z 191 and 217 fragmentograms of the oil samples are plotted in Fig. 4. Maturity increases with increasing C29Ts/C29Ts+C29 hopane, C29 αββ/(ααα+ αββ) and C27 Dia/(Dia+reg) ratios (Peters et al., 2005; Volkman et al., 1983; Zumberge, 1987). Moreover, during the maturation process, the ratios of C32 22S/(22S+22R) and C29 20S/(20S+20R) sterane rise from 0 to 0.6 and 0 to 0.55, respectively (Peters et al., 2005). In comparison to these ratios (Table 3), the Yammama Reservoir oil samples show a similar level of maturity and are in the early oil window (Fig. 5). The fact that the values of these five maturity-related biomarker ratios varied within the ranges of 0.12–0.16, 0.54–0.56, 0.12–0.2, 0.59–0.62, and 0.40–0.44, respectively, suggested a similar thermal maturity for different wells (Table 3). The

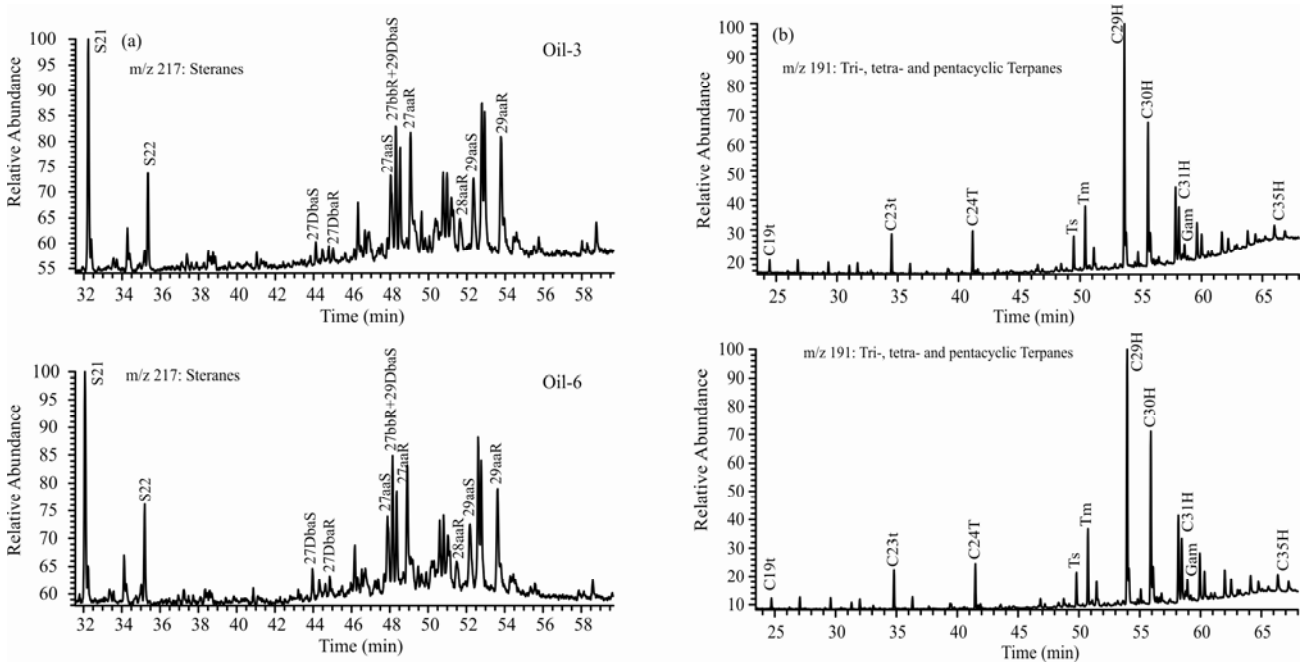

Fig. 4. (a) and (b) M/z 217 and 191 fragmentograms of two different oil samples showing the distribution of steranes and terpanes, respectively, the Yammama Reservoir in the Foroozan Oilfield.

gammacerane/C30 hopane (G/30H), C35/C34 homohopane (35HH/34HH), C29/C30 hopane (29H/30H), 24/23 tricyclic terpanes (24TT/23TT) and C24 tetracyclic terpane/C26 tricyclic terpanes (24TET/26TT) ratios are commonly used as source-related parameters (Volkman et al., 1983; Zumberge, 1987; Azevedo et al., 1992; Gürgey, 1999; Holba et al., 2003, 2001; Peters et al., 2005). The source-related biomarker parameters also showed an identical source rock for different oil samples (Table 3). Figure 6 shows the same source rock and a similar maturity level based on these aforementioned biomarker parameters of the oil samples.

4.3 Low-molecular weight hydrocarbons

Another technique used in reservoir continuity assessment is the high-resolution gas chromatography method (Kaufman et al., 1990; Smalley and Hale, 1996; Márquez et al., 2016). The ratios of small peaks between normal alkanes can be used to evaluate reservoir continuity. Patterns of low-molecular weight hydrocarbons were studied in the oil samples taken from the Yammama Reservoir, using the method suggested by Kaufman et al. (1990). Figure 7 shows the i-C_5 to n-C_9 high-resolution gas chromatograms of the oil well Nos. 3 and 6 as representative of the northwestern and southeastern parts of the Yammama Reservoir, respectively. Calculated in the next step were the whole oil gas chromatogram and six minor peak ratios including n-C_7/toluene, benzene/1,1-dimethylcyclopentane, n-C_7/methylcyclohexane, 2t-ethylmethylcyclopentane/1t,2-dimethylcyclohexane, 2,6-dimethylheptane/1,1,3-trimethylcyclohexane and m-xylene/4-methyloctane.

The star diagrams shown in Fig. 8 indicate two oil groups with significantly different values of n-C_7/toluene, 2,6-dimethylC_7/1,1,3-trimethylcycloC_6 and m-xylene/4-methylC_8 parameters: (1) the oil wells in the northwestern part of the field, and (2) the wells located in the southeastern part of the Yammama Reservoir. The two groups were separated by the fault system which prevented further fluid communication between the groups (Fig.1b). The results of high-resolution gas chromatography were consistent with other gas geochemistry results, as mentioned earlier, all of which indicated two separate compartments in the Yammama Reservoir.

4.4 Petroleum bulk properties

The values of the sulfur and asphaltene content, V/Ni ratios, and API gravities of the oil samples are given in Table 4. Despite an insignificant difference in the sulfur

Table 3 Maturity and source-related biomarker parameters at different wells drilled into theYammama Reservoir, Foroozan Oilfield

Well No.	29Ts/ (29Ts+29H)	C29 αββ/ (ααα+ αββ)	C27 Dia/ (Dia+Reg)	G/30H	35HH/ 34HH	C29H/ C30H	24TT/ 23TT	C24TET/ C26TT	C32 22S/ (22S+22R)	C29 20S/ (20S+20R)
1	0.16	0.54	0.16	0.09	1.3	1.52	0.29	7.1	0.59	0.41
2	0.13	0.55	0.12	0.08	1.29	1.63	0.25	7.16	0.61	0.4
3	0.14	0.55	0.13	0.09	1.32	1.65	0.26	7.53	0.59	0.4
4	0.12	0.55	0.15	0.07	1.22	1.57	0.29	6.07	0.6	0.43
5	0.13	0.55	0.14	0.10	1.16	1.66	0.27	6.7	0.6	0.45
6	0.13	0.56	0.2	0.05	1.06	1.62	0.25	4.22	0.61	0.45
7	0.13	0.55	0.18	0.08	0.99	1.48	0.28	5.32	0.62	0.43
8	0.12	0.55	0.16	0.07	1.10	1.53	0.3	6	0.6	0.43
9	0.12	0.56	0.17	0.06	1.25	1.61	0.26	5.38	0.62	0.44
10	0.13	0.55	0.17	0.08	1.28	1.42	0.29	6.05	0.6	0.43
11	0.12	0.55	0.16	0.08	1.25	1.52	0.29	4.77	0.61	0.42

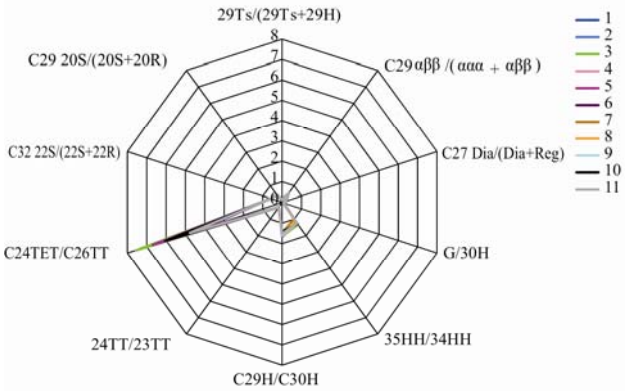

Fig. 5. Plots of C29 20S/(20S+20R) versus C32 22S/(22S+22R) sterane ratios in the Yammama Reservoir oil samples.

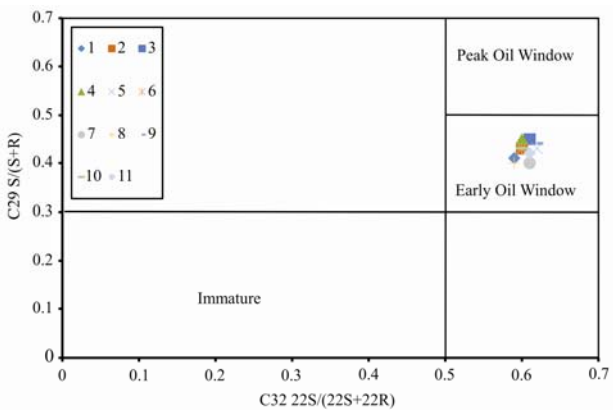

Fig. 6. Star diagram of the oil samples based on source and maturity-related biomarker parameters.

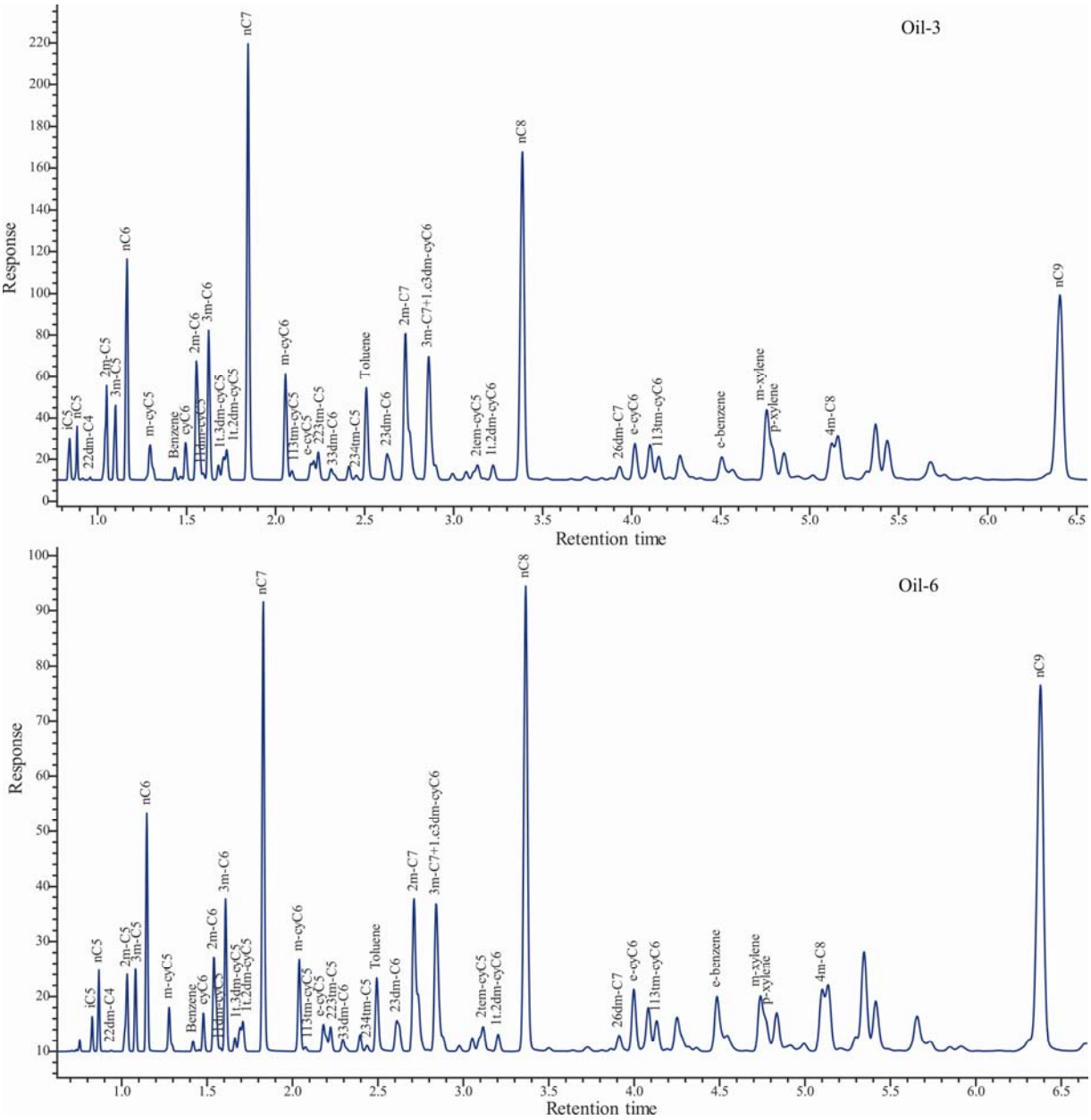

Fig. 7. High-resolution gas chromatograms for well Nos. 3 and 6, representing the northwestern and southeastern parts of the Yammama Reservoir, respectively.

content between different oil samples (on average, 2.3% in the southeastern part and 2.9% in the northwestern part of the reservoir), the asphaltene content, V/Ni ratios and API gravity of the oil samples suggested lateral heterogeneity in petroleum bulk properties.

Average API gravity values of the oil samples decreased from 38.4 in the southeastern part of the reservoir to 31.6 in the northwestern part of the reservoir. Also, the average Ni/V ratio of the oil samples decreased in a similar way from 2.3 to 1.52. Moreover, the average asphaltene content of the oil samples increased along a northward direction from 36.4 to 63.3. Trends of variations observed in the asphaltene content, V/Ni ratios and API gravity of the oil samples suggest a northward decrease in maturity. In addition to the northward decrease in maturity, there is a slight northward increase in the sulfur content of the oil samples, which was probably related to higher concentrations of polar compounds (Peters et al., 2005).

Therefore, the Yammama Reservoir shows clear compositional changes from the southern part of the field to its northern part. Based on the above-presented data, we believe that the Yammama Reservoir has been charged from the south, i.e. the source rock is deposited in the southern part of the field. Accordingly, low-maturity oils accumulated in the northern part of the reservoir and

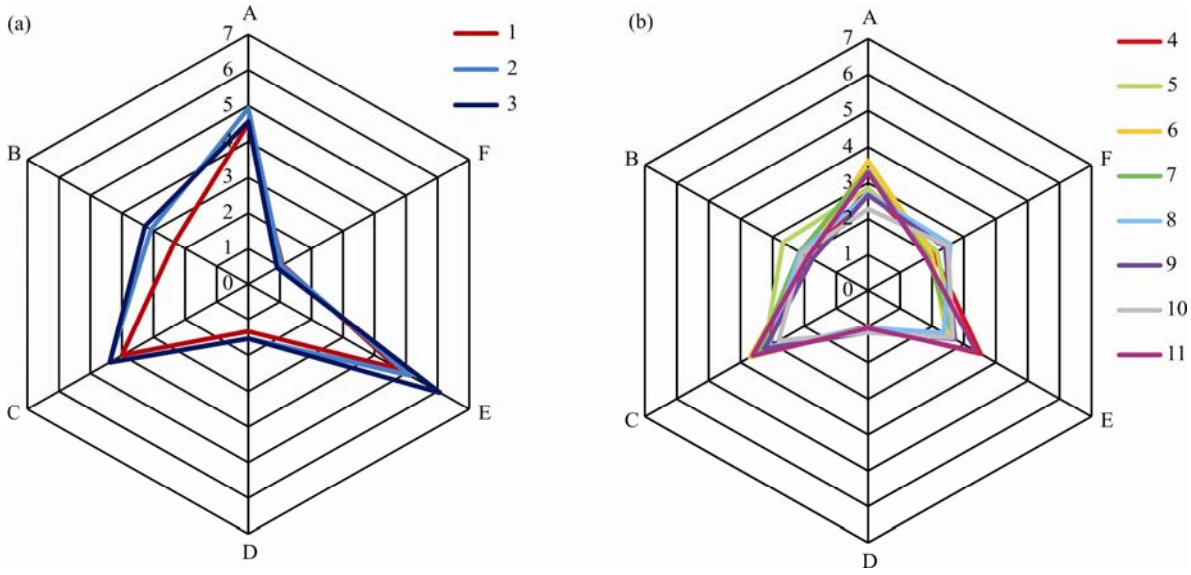

Fig. 8. Star diagrams of the northwestern (a) and southeastern parts (b) of the Yammama Reservoir, based on the peak ratios n-C_7/toluene, benzene/1,1-dimethylcyclopentane, n-C_7/methylcyclohexane, 2t-ethylmethylcyclopentane/1t,2-dimethylcyclohexane, 2,6-dimethylheptane/1,1,3-trimethylcyclohexane, and m-xylene/4-methyloctane, corresponding to the vertices A to F, respectively.

Table 4 Petroleum bulk geochemical data

Well No.	S	Asphaltene	V	Ni	V/Ni	API
1	2.5	89	13.4	5	2.7	35.9
2	3.1	53	51.4	51.8	0.99	31.5
3	3	48	16.9	19.4	0.87	27.3
4	2.3	26	18.7	8.7	2.15	39.5
5	2.3	41	21.8	9	2.42	36
6	2.1	36	11.4	5.3	2.16	48.8
7	1.4	27	13.7	6.1	2.25	40.5
8	2.9	54	22.6	11	2.05	34.5
9	2.7	39	24	10.1	2.38	34.5
10	3.1	57	28.9	12.3	2.35	31.7
11	1.9	11	10.2	3.9	2.62	41.4

Note: S is in percent, V and Ni are in ppm and asphaltene is in mg.

subsequent petroleum expulsion from the source rock kitchen have accumulated in the southern part of the reservoir.

4.5 Reservoir engineering evidence

The Foroozan Oilfield is known to be divided into five segments by geological barriers, including the F1, F2, F3, F5 and F8 segments. Well Nos. 1 to 3 are located in the F2 segment while all other wells (i.e. Well Nos. 4 to 11) have been drilled into the F3 segment. Several lines of reservoir engineering evidence support the presence of reservoir compartmentalization, as described in the following paragraphs.

The main piece of information strongly indicating compartmentalization of the Yammama Reservoir in the F2 and F3 segments is different fluid contacts. The original WOCs used to delineate the Yammama Reservoir are −8190 and −8060 ftss in the F2 and F3 segments, respectively.

Different original WOCs in the F2 and F3 segments indicate that the reservoir has been separated into two probably disconnected compartments within these areas.

The Yammama Reservoir is thought to be an originally saturated reservoir in all segments; however, considering the present reservoir pressure in the F2 segment (3250 psi) and the oil bubble point pressure (2515 psi), the Yammama Reservoir represents an under-saturated reservoir in the F2 segment.

5 Conclusions

In order to understand the continuity status of the Yammama Reservoir, a combination of geochemical and reservoir engineering studies were undertaken, and the following conclusions were drawn:

Different parts of the Yammama Reservoir in the Foroozan Oilfield are charged by the same source rock.

Two distinct petroleum groups were found in the Yammama Reservoir, separated by a fault. Demonstrated by various geochemical analyses and reservoir engineering evidence, the sealing characteristic of the fault was found to have prevented fluid communication between wells in the northwestern and southeastern parts of the reservoir.

Integrating all of the available geochemical parameters, it was concluded that the Yammama Reservoir was charged from the south.

Different original WOCs in the F2 and F3 segments and different reservoir types, in terms of saturation, comprised the main reservoir engineering evidence confirming compartmentalization of the Yammama Reservoir.

Acknowledgments

This work was financially supported by the Exploration Directorate of the National Iranian Oil Company. The authors would like to further thank the Iranian Offshore Oil Company (IOOC) and Mr. A. Yahyaei, for providing access to the samples and for his assistance, respectively. Furthermore, the Institute of Geology and Geochemistry of Petroleum and Coal, RWTH Aachen University, and GEO-data and Hydroisotop Companies are greatly appreciated for their analysis of the samples.

Manuscript received Apr. 4, 2018
accepted Jun. 5, 2018
edited by Jeff Liston and Fei Hongcai

References

ASTM, 2011. D-4052: Standard for Density, Relative Density, and API Gravity of Liquids by Digital Density Meter. In: *American Society For Testing Materials Standards.*

Azevedo, D.D.A., Neto, F.A., Simoneit, B.R.T., and Pinto, A.C., 1992. Novel series of tricyclic aromatic terpanes characterized in Tasmanian tasmanite. *Organic Geochemistry*, 18(1): 9–16.

Beeunas, M.A., Baskin, D.K., and Schoell, M., 1999. Application of gas geochemistry for reservoir continuity assessment and identification of fault seal breakdown, South Marsh Island 61, Gulf of Mexico. In *AAPG Hedberg Research Conference "Natural Gas Formation and Occurrence", Durango, Colorado*.

Chung, H.M., Gormly, J.R., and Squires, R.M., 1988. Origin of gaseous hydrocarbons in subsurface environments: theoretical considerations of carbon isotope distribution. *Chemical Geology*, 71(1–3): 97–104.

England, W.A., Muggeridge, A.H., Clifford, P.J., and Tang, Z., 1995. Modelling density-driven mixing rates in petroleum reservoirs on geological time-scales, with application to the detection of barriers in the Forties Field (UKCS). *Geological Society, London, Special Publications*, 86(1): 185–201.

England, W.A., 2007. Reservoir geochemistry-A reservoir engineering perspective. *Journal of Petroleum Science and Engineering*, 58(3–4): 344–354.

Gill, C.E., Shepherd, M., and Millington, J.J., 2010. Compartmentalization of the Nelson field, Central North Sea: evidence from produced water chemistry analysis. *Geological Society, London, Special Publications*, 347(1): 71–87.

Gürgey, K., 1999. Geochemical characteristics and thermal maturity of oils from the Thrace Basin (western Turkey) and western Turkmenistan. *Journal of Petroleum Geology*, 22(2): 167–189.

Hill, R.J., Jarvie, D.M., Zumberge, J., Henry, M., and Pollastro, R.M., 2007. Oil and gas geochemistry and petroleum systems of the Fort Worth Basin. *AAPG bulletin*, 91(4): 445–473.

Holba, A.G., Ellis, L., Dzou, I.L., Hallam, A., Masterson, W.D., Francu, J., and Fincannon, A.L., 2001. Extended tricyclic terpanes as age discriminators between Triassic, Early Jurassic and Middle-Late Jurassic oils. In *20th International Meeting on Organic Geochemistry*, 1: 464.

Holba, A.G., Zumberge, J., Huizinga, B.J., Rosenstein, H., and Dzou, L.I., 2003. Extended tricyclic terpanes as indicators of marine upwelling. In: *21st International Meeting on Organic Geochemistry, Book of Abstracts Part I,* 131.

Hovadik, J.M., and Larue, D.K., 2010. Stratigraphic and structural connectivity. *Geological Society, London, Special Publications*, 347(1): 219–242.

Hwang, R.J., and Baskin, D.K., 1994. Reservoir connectivity and oil homogeneity in a large-scale reservoir. *Geoscience Geo94*, 2: 529–541.

Internal Report of NIOC Exploration Directorate, 2017. *Geological and geophysical studies carried out on Persian Gulf and Abadan Plateau of the Islamic Republic of Iran*.

Internal Report of NIOC Exploration Directorate, 2012. Geochemical studies of Gache Turush, sulfur spring, anhydritic layers and H2S precipitation of gas reservoirs in Zagros sedimentary basin, Iran.

Kaufman, R.L., Ahmed, A.S., and Elsinger, R.L., 1990. Gas chromatography as a development and production tool for fingerprinting oils from individual reservoirs: Applications in the Gulf of Mexico. In: *GCSSEPM Foundation Ninth Annual Research Conference Proceedings,* 263–282.

Levaché, D., Montel, F., and Walgenwitz, F., 2000, January. Deep offshore fluid evaluation/connectivity study. In *SPE Annual Technical Conference and Exhibition*. Society of Petroleum Engineers.

Machel, H.G., Krouse, H.R., and Sassen, R., 1995. Products and distinguishing criteria of bacterial and thermochemical sulfate reduction. *Applied geochemistry*, 10(4): 373–389.

Márquez, G., Escobar, M., Lorenzo, E., Gallego, J.R., and Tocco, R., 2013. Using gas geochemistry to delineate structural compartments and assess petroleum reservoir-filling directions: A Venezuelan case study. *Journal of South American Earth Sciences*, 43: 1–7.

Márquez, G., Escobar, M., Lorenzo, E., Duno, L., Esquinas, N., and Gallego, J.R., 2016. Intra-and inter-field compositional changes of oils from the Misoa B4 reservoir in the Ceuta Southeast Area (Lake Maracaibo, Venezuela). *Fuel*, 167: 118–134.

Páez, R.H., Lawerence, J.J., and Zhang, M., 2010. Compartmentalization or gravity segregation? Understanding and predicting characteristics of near-critical petroleum fluids. *Geological Society, London, Special Publications*, 347(1): 43–53.

Permanyer, A., Douifi, L., Lahcini, A., Lamontagne, J., and Kister, J., 2002. FTIR and SUVF spectroscopy applied to reservoir compartmentalization: a comparative study with gas chromatography fingerprints results. *Fuel*, 81(7): 861–866.

Permanyer, A., Rebufa, C., and Kister, J., 2007. Reservoir compartmentalization assessment by using FTIR spectroscopy. *Journal of Petroleum Science and Engineering*, 58(3–4): 464–471.

Peters, K.E., Walters, C.C., and Moldowan, J.M., 2005. The Biomarker guide, biomarkers and isotopes in petroleum exploration and earth history, vol. 1–2.

Prinzhofer, A., Mello, M.R., da Silva Freitas, L.C., and Takaki, T., 2000. New geochemical characterization of natural gas and its use in oil and gas evaluation . In: *AAPG Memoir 73, Chapter 9*.

Rein, E., and Schulz, L.K., 2007. Applications of natural gas tracers in the detection of reservoir compartmentalisation and production monitoring. *Journal of Petroleum Science and Engineering*, 58(3–4): 428–442.

Rooney, M.A., 1996. Carbon isotopic evidence for the accelerated destruction of light hydrocarbons by thermochemical sulfate reduction. In: *1996 NSERC Thermochemical Sulphate Reduction (TSR) and Bacterial Sulphate Reduction (BSR) Workshop*. University of Calgary.

Schoell, M., 1983. Genetic characterization of natural gases. *AAPG bulletin*, 67(12): 2225–2238.

Schoell, M., Jenden, P.D., Beeunas, M.A., and Coleman, D.D., 1993. January. Isotope analyses of gases in gas field and gas storage operations. In: *SPE Gas Technology Symposium*. Society of Petroleum Engineers.

Smalley, P.C., and Hale, N.A., 1996. Early identification of reservoir compartmentalization by combining a range of conventional and novel data types. *SPE Formation Evaluation*, 11(03): 163–170.

Volkman, J.K., ALExANDER, R.O.B.E.R.T., Kagi, R.I., Noble, R.A., and Woodhouse, C.W., 1983. A geochemical reconstruction of oil generation in the Barrow Sub-basin of Western Australia. *Geochimica et Cosmochimica Acta*, 47 (12): 2091–2105.

Vrolijk, P., 2005. Reservoir Connectivity Analysis-Defining Reservoir Connections & Plumbing. In *SPE Middle East Oil and Gas Show and Conference*. Society of Petroleum Engineers.

Whiticar, M.J., Faber, E., and Schoell, M., 1986. Biogenic methane formation in marine and freshwater environments: CO_2 reduction vs. acetate fermentation—isotope evidence. *Geochimica et Cosmochimica Acta*, 50(5): 693–709.

Worden, R.H., Smalley, P.C., and Oxtoby, N.H., 1995. Gas souring by thermochemical sulfate reduction at 140 C. *AAPG Bulletin*, 79(6): 854–863.

Worden, R.H., Smalley, P.C., and Cross, M.M., 2000. The influence of rock fabric and mineralogy on thermochemical sulfate reduction: Khuff Formation, Abu Dhabi. *Journal of Sedimentary Research*, 70(5): 1210-1221.

Xie, Z., Li, J., Li, Z., Guo, J., Li, J., Zhang, L., and Dong, C., 2017. Geochemical characterization of the upper Triassic Xujiahe Formation in Sichuan Basin, China and its significance for hydrocarbon accumulation. *Acta Geologica Sinica* (English Edition), 91(5): 1836–1854.

Zumberge, J.E., 1987. Terpenoid biomarker distributions in low maturity crude oils. *Organic Geochemistry*, 11(6): 479-496.

Zhu, G., Zhang, S., Liang, Y., Dai, J., and Li, J., 2005. Isotopic evidence of TSR origin for natural gas bearing high H_2S contents within the Feixianguan Formation of the northeastern Sichuan Basin, southwestern China. *Science in China Series D: Earth Sciences*, 48(11): 1960–1971.

About the first author

Payam HASSANZADEH, male, born in 1985 in Fereydoonkenar City, Mazandaran Province, Iran; PhD student of petroleum exploration engineering, Amirkabir University of Technology; he is currently interested in the study of reservoirs, and time-lapse geochemistry. Email:payamhasanzade@gmail.com; phone: 0098-9363883534, 0098-2144751863.